

pubs.acs.org/acscatalysis Research Article

# Controllable Multihalogenation of a Non-native Substrate by the SyrB2 Iron Halogenase

R. Hunter Wilson, Sourav Chatterjee, Elizabeth R. Smithwick, Anoop R. Damodaran,\* and Ambika Bhagi-Damodaran\*



Cite This: ACS Catal. 2024, 14, 13209-13218



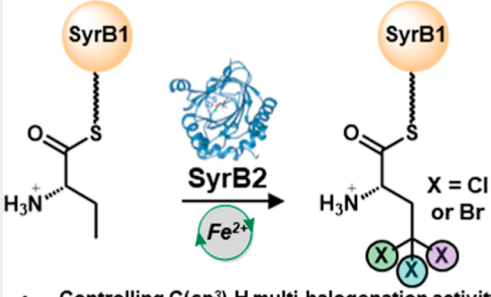
**ACCESS** I

Metrics & More

Article Recommendations

Supporting Information

ABSTRACT: Geminal, multihalogenated functional groups are widespread in natural products and pharmaceuticals, yet no synthetic methodologies exist that enable selective multihalogenation of unactivated C-H bonds. Biocatalysts are powerful tools for late-stage C-H functionalization as they operate with high degrees of regio-, chemo-, and stereoselectivity. 2-Oxoglutarate (2OG)dependent nonheme iron halogenases chlorinate and brominate aliphatic C-H bonds and offer a solution for achieving these challenging transformations. Here, we describe the ability of a nonheme iron halogenase, SyrB2, to controllably halogenate a non-native substrate  $\alpha$ -aminobutyric acid (Aba) to yield monochlorinated, dichlorinated, and trichlorinated products. These chemoselective outcomes are achieved by controlling the loading of the 2OG cofactor and SyrB2 biocatalyst. Furthermore, by using a ferredoxin-based biological reductant for electron transfer to the catalytic center of SyrB2, we demonstrate



- Controlling C(sp³)-H multi-halogenation activity
- Molecular insights into chemoselectivity
- Proof-of-concept synthetic utility

order-of-magnitude enhancement in the yield of trichlorinated products that were previously inaccessible using any single halogenase enzyme. We also apply these strategies to broaden SyrB2's reactivity scope to include multibromination and demonstrate chemoenzymatic conversion of the ethyl side chain in Aba to an ethynyl functional group. We show how steric hindrance induced by the successive addition of halogen atoms on Aba's  $C_4$  carbon dictates the degree of multihalogenation by hampering  $C_3$ – $C_4$  bond rotation within SyrB2's catalytic pocket. Overall, our work showcases the potential of iron halogenases to facilitate multi-C-H functionalization chemistry.

KEYWORDS: 20G-dependent, C-H functionalization, halogenation, nonheme-iron, multihalogenation

# **■ INTRODUCTION**

Achieving direct and selective functionalization of aliphatic C-H bonds poses significant challenges for organic synthesis. Biocatalysis has emerged as a solution to this problem as enzymes offer regio-, stereo-, and chemoselective functional group installation in large yields. 1 Nonheme iron enzymes, specifically those which require a 2-oxoglutarate (2OG) cofactor, are of specific interest due to their incredibly diverse reaction scope which includes epimerization,<sup>2</sup> hydroxylation,<sup>3,4</sup> desaturation, <sup>5-7</sup> epoxidation, <sup>8-10</sup> and aziridination. <sup>11</sup> Notably, 20G-dependent nonheme iron halogenases (hereafter referred to as iron halogenases) can perform chlorination, 12,13 dichlorination, 14-20 and bromination 14,16,21-23 on unactivated C-H bonds of their native substrates, though all of these reactions compete with a hydroxylation side reaction. The most extensively researched class of iron halogenases are the ACP-dependent halogenases which require delivery of their substrates by covalent attachment to a phosphopantetheinyl (Ppt) group appended to an acyl-carrier protein (ACP). 12,13,15,19-22,24 In recent years, free-standing halogenases have also been discovered that bind and halogenate substrates in their active sites without the need of an

ACP. 16,25,26 Iron halogenases have been identified to be responsible for the incorporation of monochlorinated, dichlorinated, or trichlorinated functional groups in a variety of natural products (Figure 1a). Many of these natural sparking substantial research interest in recent decades. 18,24,27-29

To date, no synthetic methodologies exist for direct multihalogenation of unactivated C-H bonds.30-35 Existing methods for multihalogenation almost always act upon  $\pi$  bonds from alkenes/alkynes<sup>36–45</sup> and activated C–H bonds from ketones<sup>46–48</sup> or require multistep synthesis<sup>49</sup> and few offer chemoselectivity toward the degree of halogenation. 33,49-58 In this work, we demonstrate systematic control of the degree of regioselective halogenation of a non-native

Received: May 12, 2024 Revised: July 27, 2024 Accepted: August 12, 2024 Published: August 19, 2024





# b This work: Controlling multi-halogenation activity in SyrB2 iron halogenase

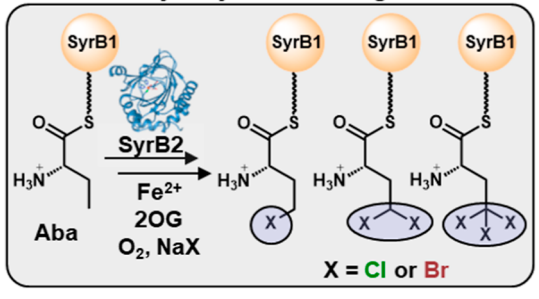


**Figure 1.** (a) Halogenated natural products containing a variety of  $C-Cl_n$  bonds, where n ranges from 1 to 3. Enzymes responsible for halogenated product formation are given under the compound name. (b) This work demonstrates chemoselective control of C-H functionalization from mono- to trihalogenation. This is achieved in a nonheme iron halogenase SyrB2 with a SyrB1-Ppt-Aba substrate.

substrate  $\alpha$ -aminobutyric acid (Aba) by the SyrB2 halogenase to yield mono-, di-, and trichlorinated products. Using molecular dynamics (MD) simulations, we explore the molecular basis for the observed reactivity patterns and highlight the role of rotational flexibility of Aba within the SyrB2 catalytic pocket on the degree of halogenation. By using a ferredoxin-based biological reductant for electron transfer to the catalytic center of SyrB2, we demonstrate order-ofmagnitude enhancement in the yield of trichlorinated products that were previously inaccessible using any single halogenase enzyme. We also reveal the ability of SyrB2 to perform di- and tribromination reactions and a potential application of geminal dibrominated Aba by converting it to an alkyne functional group useful for biorthogonal chemistry applications. Overall, our results offer new insights into controlling iron halogenase catalysis and expand its functionalization capabilities.

### ■ RESULTS AND DISCUSSION

Controlling Mono- vs Dichlorination in the SyrB2 Halogenase Using 2OG Loading. We began our studies by investigating the reactivity of SyrB1-Ppt-conjugated Aba (SyrB1-Ppt-Aba) with SyrB2 in the presence of varying equivalents of 2OG. The assay involves incubating SyrB2 with substrate SyrB1-Ppt-Aba and cofactors iron, 2OG, chloride, and O<sub>2</sub>. The unreacted or functionalized Aba is subsequently released from SyrB1-Ppt-Aba via reaction with a thioesterase and derivatized with 6-aminoquinolyl-n-hydroxysuccinimidyl carbamate (AQC) tag for ultra-performance liquid chromatography (UPLC) separation and mass spectrometric analysis by multiple reaction monitoring (MRM). As

expected, the reaction of SyrB1-Ppt-Aba with SyrB2 in the absence of 2OG yielded no products underscoring the need of the 2OG cofactor to jumpstart catalysis via formation of a chloroferryl intermediate (Figure 2a, Figures S1-S3). However, the addition of 0.5 equiv of 2OG yielded <1% monochlorinated Aba (Cl-Aba) as a reaction product. We reasoned that the conversion to Cl-Aba could be low due to an intramolecular lactonization reaction, which has been demonstrated to be occurring in halogenated products with other nonheme iron enzymes (Figure 2a, inset). 14,16,59 Subsequent UPLC/MRM studies validated such expectations with the major reaction product appearing in the MRM channel corresponding to the lactonized form of Aba (Lac-Aba) and were later confirmed via accurate mass measurements (Figures 2a and S4-S6). Moreover, by enhancing the 2OG cofactor to 1 and 2.5 equiv with respect to the substrate, we achieve 33 and 41% conversion to the monochlorinated Aba product (Lac-Aba + Cl-Aba), respectively. Intriguingly, with these reaction conditions, we also start to observe the formation of a product whose mass corresponds to dichlorinated Aba (Cl<sub>2</sub>-Aba) (Figure S7). We reasoned that the dichlorination of Aba could be happening by a second chlorination reaction on Aba's C<sub>4</sub> carbon. To validate this hypothesis and increase the conversion to the dichlorinated product, we increased the loading of the 2OG cofactor. Indeed at 5 equiv 2OG loading, we achieve a conversion of up to 97% Cl<sub>2</sub>-Aba while decreasing Lac-Aba and Cl-Aba to a combined 1.7% conversion (Figures 2a and S8). Unlike Cl-Aba, Cl<sub>2</sub>-Aba appears to be resistant to intramolecular cyclization. We attribute this to the additional steric hindrance of a second chlorine atom on C4 that would prevent lactonization. As we further increased the 2OG loading to 10 and 100 equiv, we also began to observe masses that correspond to a trichlorinated product (Cl<sub>3</sub>-Aba, up to 9% conversion) (Figures S8-S10) that correlated with a decrease in conversion to Cl<sub>2</sub>-Aba (decreased to 87% conversion) (Figure 2a). To confirm the identities of these analytes as Cl<sub>2</sub>-Aba and Cl<sub>3</sub>-Aba, we performed accurate mass measurements on our reaction products. These studies showed that the theoretical isotopic [M + H]<sup>+</sup> distributions of Cl<sub>2</sub>-Aba and Cl<sub>3</sub>-Aba match those exhibited by the experimental isotopic distributions (Figure S11). Moreover, the mass error between the theoretical and experimental monoisotopic masses is 2.3 ppm for Cl<sub>2</sub>-Aba and 1.6 ppm for Cl<sub>3</sub>-Aba, validating their identity. Overall, by systematic tuning of 2OG loading, we demonstrate controlled mono- vs dichlorination of Aba by SyrB2.

While our accurate mass studies confirmed the identities of Cl<sub>2</sub>-Aba and Cl<sub>3</sub>-Aba, we wanted to structurally characterize the reaction products. More specifically, we wanted to confirm that the C<sub>4</sub> position was the site where all of the new C-Cl bonds were formed. Given the small scale of our reactions and our existing detection by MS, we opted to use a deuterated substrate to probe the site-selectivity of the reaction. By appending 3,3-D<sub>2</sub>-Aba to SyrB1-Ppt and monitoring the chlorination assay products via MS, we would be able to detect how many deuterium atoms were retained in the Cl<sub>2</sub>-Aba product (Figure 2b). If the Cl<sub>2</sub>-Aba product contained only a single deuterium atom, then we could infer that one chlorine atom was incorporated at C3, while the other was incorporated at C4. If both deuterium atoms were retained, then all C-Cl bonds would be formed at position C4, forming a geminal dichlorinated product. In turn, we performed the chlorination assay with the SyrB1-Ppt-3,3-D<sub>2</sub>-Aba substrate

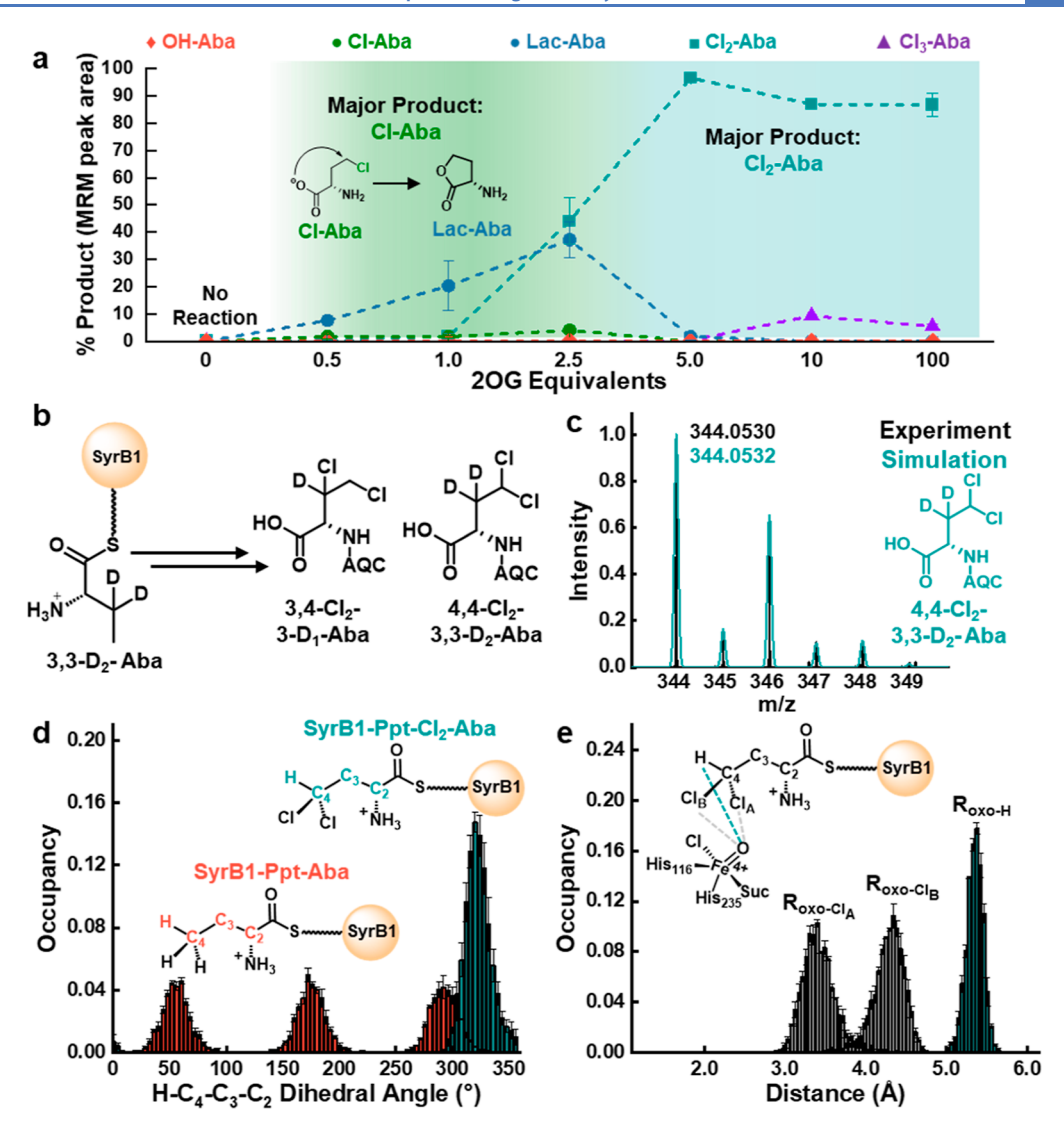


Figure 2. (a) AQC-tagged products detected as a percentage of total MRM peak area for SyrB2's reaction with SyrB1-Ppt-Aba at varied 2OG loading. Error bars are the standard deviation from n = 3 reactions. The % MRM peak area reflects trends in product selectivity and not definitive molar ratios. (b) For a dichlorinated product, the chlorine atoms can either install on  $C_4$  or on  $C_3$  and  $C_4$ . By conducting the reaction with a deuterated substrate probe, either both or a single deuterium can be retained on  $C_3$ . (c) Experimental high-resolution mass spectrometry (HR-MS) spectrum of the  $Cl_2$ -Aba product from the chlorination reaction of 3,3-D<sub>2</sub>-Aba overlaid with the simulated spectrum for 4,4, $Cl_2$ -3,3-D<sub>2</sub>-Aba. (d) MD simulation results monitoring the  $H-C_4-C_3-C_2$  dihedral angle of the SyrB1-Ppt-Aba and SyrB1-Ppt-Cl<sub>2</sub>-Aba substrates in the SyrB2 active site. (e) MD simulation results monitoring the  $C_4$  chlorine and hydrogen atom distances of SyrB1-Ppt-Cl<sub>2</sub>-Aba to the oxo ligand of the chloroferryl intermediate in the SyrB2 active site. MD error bars are the standard error across three independent production runs. Suc = succinate.

and probed the identity of Cl2-products using accurate mass measurements. When comparing our experimental result for the dichlorinated product with 3,4,Cl<sub>2</sub>-3-D<sub>1</sub>-Aba, we see a poor fit to the isotopic distribution pattern and a monoisotopic mass error of 2933 ppm (Figure S12). On the other hand, when comparing with the simulated mass spectrum in which both deuterium atoms are retained (4,4-Cl<sub>2</sub>-3,3-D<sub>2</sub>-Aba), we observe excellent agreement with the isotopic distribution pattern and a monoisotopic mass error of 0.6 ppm (Figure 2c). These observations support that both deuterium atoms were retained, and all chlorine atoms were installed at position C<sub>4</sub>. Next, we wanted to confirm that C<sub>4</sub> was the position at which all three chlorine atoms were being installed for the Cl<sub>3</sub>-Aba product as well. Upon comparing the experimental mass spectrum to the simulated spectrum of 3,4,4-Cl<sub>3</sub>-3-D<sub>1</sub>-Aba, a poor fitting to the isotopic pattern is observed, and the monoisotopic mass error is 2671 ppm (Figure S13). When

overlaying the experimental spectrum and the simulated spectrum for 4,4,4-Cl<sub>3</sub>-3,3-D<sub>2</sub>-Aba, we see an excellent agreement between the experimental and simulated isotopic patterns and a monoisotopic mass error of 1.6 ppm (Figure S13). This result shows that both deuterium atoms were retained during the assay, and all three chlorine atoms were installed at the C<sub>4</sub> position. Overall, these studies demonstrate that SyrB2 can regioselectively multichlorinate Aba to produce geminal di- and trichlorinated products.

Influence of Substrate C–C Bond Rotational Flexibility on the Degree of Chlorination. Our results so far demonstrate that chlorination reactions with equimolar SyrB1-Ppt-Aba and SyrB2 in the presence of excess 2OG yield dichlorinated Aba with high selectivity (Figure 2a). Density functional theory (DFT) bond dissociation energy calculations reveal that C–H bond energy at the C<sub>4</sub> position of Aba is lowered upon successive chlorination reactions, suggesting that

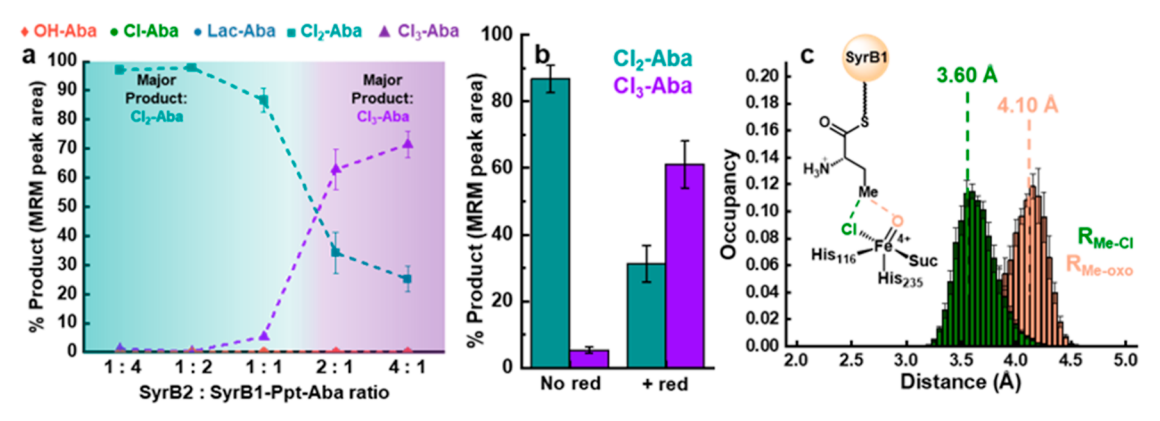


Figure 3. (a) AQC-tagged products detected as a percentage of total MRM peak area for SyrB2's reaction with SyrB1-Ppt-Aba at varied SyrB2 biocatalyst loading. No AQC-tagged monochlorinated, lactonized, or hydroxylated Aba analytes were detected in the assays. The 2OG loading was set to 100 equiv; error bars are the standard deviation from n = 3 reactions. (b) AQC-tagged products detected as a percentage of total MRM peak area for SyrB2's reaction with SyrB1-Ppt-Aba without and with the biological reductant (abbreviated as red). The substrate to catalyst loading ratio was kept at 1:1, and the 2OG loading was set to 100 equiv. Error bars are the standard deviation from n = 3 reactions. The % MRM peak area in (a-b) reflects trends in product selectivity and not definitive molar ratios. (c) MD simulations of the SyrB2/SyrB1-Ppt-Aba complex with the reactive chloroferryl intermediate show that the reactive carbon is positioned closer to the halide ligand, favoring a halogenation outcome; error bars are the standard error over three independent production runs, and vertical lines indicate the distance at which 50% of the distribution occurs.

bond strength is not a factor for hindered multichlorination (Figure S14). To understand why a third chlorination reaction at the C<sub>4</sub> position is disfavored, we investigated the molecular basis for the degree of chlorination. For a chlorination reaction to proceed, the hydrogen atoms on Aba's C<sub>4</sub> must approach distances proximal to the oxo ligand of the reactive chloroferryl intermediate so that they can be abstracted (Figure S3). We hypothesized that the addition of two chlorine atoms to the C<sub>4</sub> of Aba would introduce significant steric bulk and alter the conformational positioning of the substrate in the active site, disfavoring the third H atom abstraction needed to form Cl<sub>3</sub>-Aba. We explored this hypothesis by performing MD simulations of SyrB2 with both the SyrB1-Ppt-Aba and SyrB1-Ppt-Cl<sub>2</sub>-Aba substrates. First, we compared the rotational flexibility of the C<sub>3</sub>-C<sub>4</sub> bond between the two substrates by observing the  $H-C_4-C_3-C_2$  dihedral angle (Figures 2d and S15). For SyrB1-Ppt-Aba, we observe three distinct dihedral distributions, indicating facile rotation about the C<sub>3</sub>-C<sub>4</sub> bond in the SyrB2 active site. When comparing the distance distributions between the SyrB1-Ppt-Aba C4 hydrogens and the oxo ligand, we observe that they all overlay and can approach distances within <3.0 Å of the oxo ligand (Figure S16). This implies that any of the hydrogens of SyrB1-Ppt-Aba can be easily abstracted to form a monochlorinated product. In contrast to the nonfunctionalized Aba substrate, SyrB1-Ppt-Cl<sub>2</sub>-Aba only has a single dihedral distribution, indicating that the C<sub>3</sub>-C<sub>4</sub> bond is not rotatable, and the substrate is locked into a single dihedral conformation (Figure 2d). As a result, when we monitor the distance distribution between the C<sub>4</sub>'s chlorine and hydrogen atoms to the oxo ligand, each has a distinct distribution (Figure 2e). While the chlorine atoms are more proximal to the oxo ligand (4.5 Å or less; shaded gray), the last abstractable hydrogen atom is located ~5.5 Å from the oxo ligand (shaded cyan). At these longer distances, H atom abstraction would be greatly impeded,60 which could explain hindered production of Cl<sub>3</sub>-Aba in our assays. In turn, the MD simulations suggest that steric effects upon successive chlorination can impact the optimal positioning of the substrate's C<sub>4</sub> hydrogen and may require multiple binding events, thereby hindering trichlorination. While these analyses provide context for our observed reactivity, we were also

curious as to whether the protein environment provided a means for product release. Further calculations on our trajectories revealed a potential tunnel for gas diffusion created by the SyrB1-Ppt arm and SyrB2 residues Gly194, Phe195, and Phe196 (Figure S17). The nonpolar lining of this tunnel could provide facile access for diffusion of  $O_2/CO_2$  from the SyrB2 active site. To enable the release of the other products, large-scale changes in the SyrB2 tertiary structure would have to occur to release succinate and break SyrB1/SyrB2 protein—protein interactions, which the time scales of our simulations would not capture. Overall, our studies reveal that the steric bulk caused by the subsequent addition of chlorine atoms on the substrate can severely impede  $C_3-C_4$  bond rotation in the SyrB2 active site and dictates the degree of multichlorination reactivity.

Enhanced Geminal Trichlorinated Product Yields with Ferredoxin as a Biological Reductant. The ability to obtain ~9% Cl<sub>3</sub>-Aba in our halogenase assays was an exciting reaction outcome as no sole enzyme has been shown to directly trichlorinate a substrate, let alone one with unactivated, aliphatic C-H bonds. Notably, the biosynthesis of a geminal trichlorinated functional group of barbamide requires the action of two independent iron halogenases, BarB1 and BarB2. More specifically, while BarB2 dichlorinates the unactivated C5 carbon of the leucine substrate (attached to BarA-Ppt ACP) (Figure 1a), BarB1 completes the third chlorination step to yield the final trichlorinated product. In an effort to increase the yield of Cl<sub>3</sub>-Aba in our assays, we systematically varied the catalyst: substrate ratio (SyrB2: SyrB1-Ppt-Aba) (Figure 3a). When the substrate is in excess of the catalyst (SyrB2: SyrB1-Ppt-Aba ratios of 1:4 and 1:2), we observe Cl<sub>2</sub>-Aba as the primary product with >98% conversion, revealing how selective the enzyme is toward dichlorination. At an equimolar catalyst: substrate ratio, however, we start to observe the appearance of ~5% Cl<sub>3</sub>-Aba, and the conversion of Cl<sub>2</sub>-Aba decreases to 87%. When we overload the amount of catalyst with respect to the substrate (SyrB2: SyrB1-Ppt-Aba ratios of 2:1 and 4:1), we observe significant amounts of the trichlorinated product. Notably, at a catalyst: substrate ratio of 4:1, we observe as high as 72% of Aba converted to Cl<sub>3</sub>-Aba, with only 25% converted

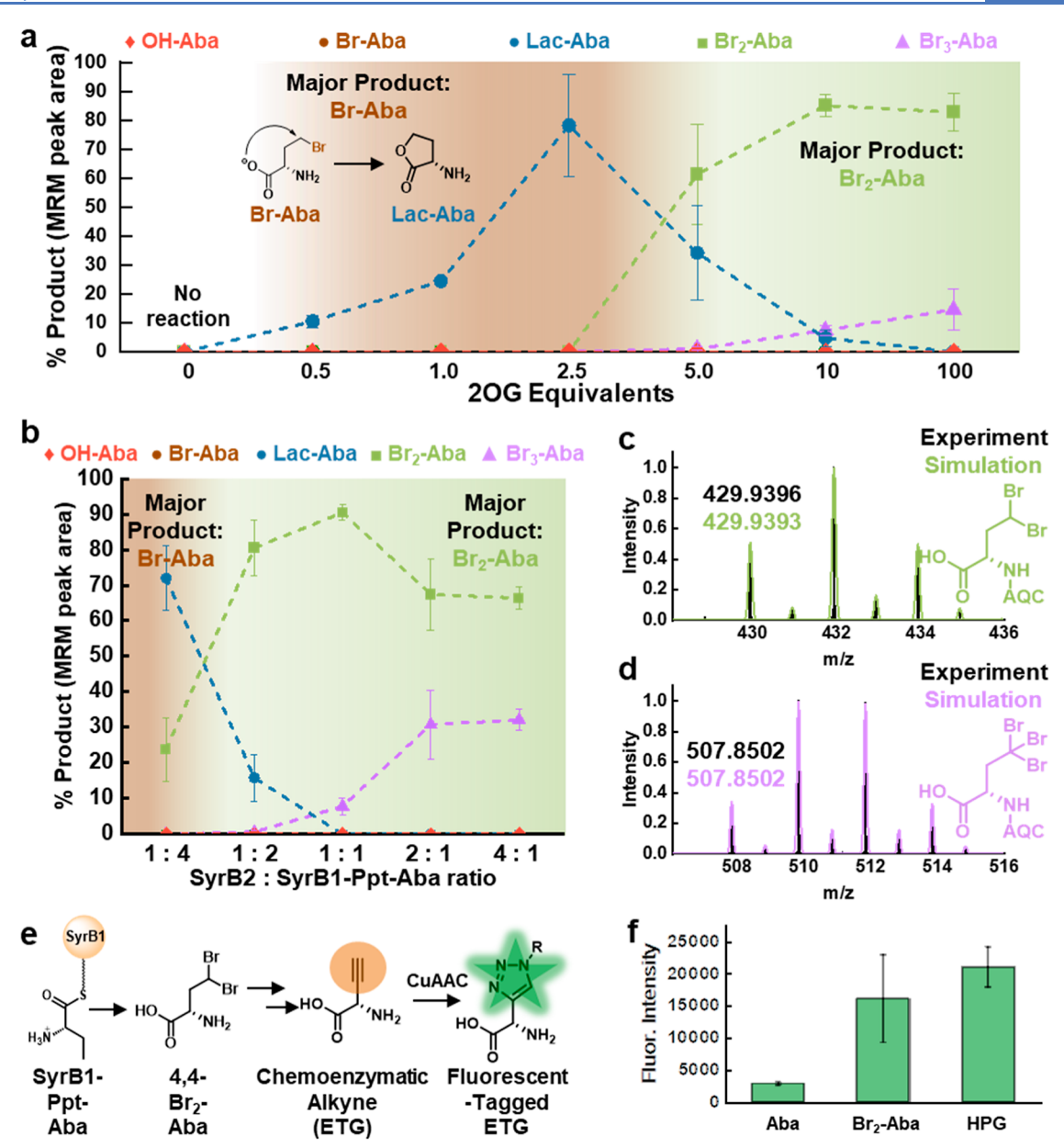


Figure 4. Iron halogenase catalyzed multibromination activity and demonstrated synthetic utility. AQC-tagged products detected as a percentage of total MRM peak area for SyrB2's reaction with SyrB1-Ppt-Aba at varied (a) 2OG loading and (b) varied SyrB2 biocatalyst loading. Error bars are the standard deviation from n = 3 reactions. The % MRM peak area in (a–b) reflects trends in product selectivity and not definitive molar ratios. (c) HR-MS spectrum validating Br<sub>2</sub>-Aba identity. (d) HR-MS spectrum validating Br<sub>3</sub>-Aba identity. (e) Overview for the chemoenzymatic conversion of Aba to ethynylglycine (ETG) and its detection via click chemistry assay. (f) Fluorescence responses demonstrating chemoenzymatic alkyne formation from Br<sub>2</sub>-Aba and a 10  $\mu$ M homopropargylglycine standard. Error bars are the standard deviation from three independent reactions/assays.

to  $\text{Cl}_2\text{-Aba}$  (Figure 3a). We believe that the need for the excess catalyst-complex for the trichlorination reaction arises from the limited turnover number of  $7\pm2$  for SyrB2 before inactivation. MD simulations have shown that the dichlorinated substrate, SyrB1-Ppt-Cl2-Aba, is locked in a dihedral conformation which can impede the third H atom abstraction (Figure 2d,e). In turn, SyrB1-Ppt-Cl2-Aba bound to SyrB2 in an unfavorable locked single-dihedral conformation will need to disassociate from its partner and subsequently bind to an active SyrB2 in a dihedral conformation that is favorable for trichlorination. The opportunity for this to occur is significantly enhanced in the presence of excess catalyst. We reasoned that the low turnover for SyrB2 is likely related to

inactivation via Fe<sup>2+</sup> oxidation, a common uncoupling pathway in 2OG-utilizing iron enzymes. Such inactivation can be countered using a reductant, such as ascorbate, to reduce oxidized iron. However, ascorbate can also perform a nucleophilic attack on the thioester moiety of SyrB1-Ppt-Aba to release the tethered amino acid from the Ppt arm. Consequently, all assays with ACP-dependent halogenases to date have been conducted without a reductant. To address this challenge, we used a biological ferredoxin-based reductant system. With a significantly low redox potential of –410 mV, ferredoxin is anticipated to reduce inactivated SyrB2 and bring it back in the catalytic cycle. Indeed, in the presence of ferredoxin, we observe an 11-fold enhancement in Cl<sub>3</sub>-Aba

yields with as high as 61% of Aba converted to Cl<sub>3</sub>-Aba and with 31% converted to Cl<sub>2</sub>-Aba at a catalyst: substrate ratio of 1:1 (Figure 3b). Overall, these results along with our computational findings help understand what factors enable or limit trichlorination reactions in iron halogenases.

Molecular Basis for Chlorination over Hydroxylation with a Non-native Aba Substrate. To establish a molecular basis for our chemoselective chlorination outcome, we conducted MD simulations of the SyrB2/SyrB1-Ppt-Aba complex. We modeled the reactive chloroferryl intermediate in the SyrB2 active site as a distorted five-coordinate chloroferryl isomer with the oxo and chloro ligands in the equatorial plane as spectroscopically identified previously and monitored the distances between the reactive carbon center (C<sub>4</sub>) and the oxo and chloro ligands.<sup>65</sup> As classical MM force fields fail to describe the substrate's proper orientation about the nonheme iron center, we also applied harmonic restraints to enforce appropriate iron-Aba distances and Aba-iron-oxo angles. 60,62,70,79 Halogenases tend to organize the reactive carbon of their substrates closer to the halide ligand to favor rebound with the halogen upon H atom abstraction by the haloferryl intermediate (Figure S3). 62,65,68-80 We observe that the reactive methyl group of Aba orients itself 0.5 Å closer to the chloride ligand than the oxo ligand over 1.5  $\mu$ s of simulations (Figure 3c). This preference in distance distribution suggests that SyrB1-Ppt-Aba is positioned for a halogenation outcome over hydroxylation, which is validated by our experimental results (Figures 2a and 3a). In our studies, the MRM channels corresponding to OH-Aba show negligible peaks with no difference between the reactions of SyrB1-Ppt-Aba with SyrB2 and those without SyrB2, indicating chemoselective chlorination of Aba by SyrB2. We note that we have employed a thioesterase, TycF, for liberating Aba which is a well-established method for releasing amino acids tethered to the Ppt arm across various ACPs. 13,14,19,81-8 Previous studies that suggested similar propensity of Aba to halogenate and hydroxylate did not discuss the potential for cyclization of Cl-Aba or the potential for other side products (including OH-Aba) from the basic conditions of hydroxylamine derivatization (Figure S18).<sup>60,85</sup>

Multibromination Activity of SyrB2. Thus far, we have demonstrated control over the degree of multichlorination; however, iron halogenases are also capable of monobrominating their native substrates. 14,16,23,59,73 Given the propensity for the SyrB1-Ppt-Aba substrate to form multichlorinated products, next, we investigated if this reactivity could be extended to multibromination. We note that multibromination reactions are harder to accomplish as H-abstraction, ferryl decay, and radical rebound are all rendered slower for bromination as compared to that for chlorination.<sup>22,86,87</sup> As such, there are no previous reports of di- and tribromination by iron halogenases. To characterize bromination activity, we applied methods for controlling selectivity that were described above for multichlorination. First, we tested how the equivalents of the 2OG cofactor affected the percent conversion for all products (Figures 4a and S19-S25). In the absence of 2OG, no products were observed, indicating that the addition of 2OG is required to initiate catalysis. Upon increasing the addition of 2OG up to 2.5 equiv, the Lac-Aba product becomes the dominant product. Akin to the chlorination reaction, Lac-Aba forms from an intramolecular S<sub>N</sub>2 reaction in which the carboxylate group attacks the C–Br bond (Figure 4a, inset). Unlike the chlorination reactions,

however, no monobrominated product (Br-Aba) was observed likely due to bromide being a better leaving group than chloride for the lactonization reaction. As we increased the 2OG loading to 5 equiv, a product with masses corresponding to dibrominated Aba (Br<sub>2</sub>-Aba) became the major product, with a still appreciable amount of Lac-Aba present. In our chlorination assays, the Cl<sub>2</sub>-Aba product became the major product after adding 2.5 equiv of 2OG and was the dominant product after adding 5 equiv (Figure 2). Since bromination is not the native reaction for SyrB2, it appears that bromination operates slower than chlorination as seen in kinetics assays with iron halogenases, 21,22,86,87 leading to a lower percent conversion to multibrominated products. By adding 10 equiv of 2OG, we are able to increase the conversion of Br<sub>2</sub>-Aba up to 85%, concomitant with a decrease in Lac-Aba (and thereby Br-Aba). At 10 equiv of 2OG, a product with masses consistent with a tribrominated product (Br<sub>3</sub>-Aba) begins to appear. By increasing the 2OG loading to 100 equiv, we increase the conversion of Br<sub>3</sub>-Aba up to 10%. Overloading 2OG at this amount also eliminates signals associated with Lac-Aba, thereby fully shifting the chemoselectivity to multibrominated Aba. Analogous to our chlorination assays, negligible OH-Aba was detected at any amount of 2OG loading during these assays. Beyond 2OG, it is possible that varying the concentration of other cosubstrates such as O2 and halide could control halogenation product distribution. Overall, our studies reveal the ability to modulate chemoselectivity between mono- and multichlorinated/brominated products by altering the levels of the 2OG cofactor present in the halogenation reaction.

In an attempt to increase the conversion to Br<sub>3</sub>-Aba, we again varied the biocatalyst loading by altering the ratio of SyrB2: SyrB1-Ppt-Aba (Figure 4b). At a catalyst: substrate ratio of 1:4, we observe Lac-Aba as the dominant product at 72% conversion, while Br<sub>2</sub>-Aba is the minor product at 24% conversion. This contrasts with our chlorination studies that revealed Cl<sub>2</sub>-Aba as the major product (>95%) at a 1:4 catalyst: substrate ratio, suggesting the lower potency for multiturnovers with bromide as compared to that with chloride. However, as we increase the catalyst loading for bromination with catalyst: substrate ratios of 1:2 and 1:1, we start observing Br<sub>2</sub>-Aba as the major product with as high as 90% conversions. Finally, when the catalyst is in excess of the substrate with catalyst: substrate ratios of 2:1 and 4:1, we increase the conversion of Br<sub>3</sub>-Aba up to 32%, which is notable but considerably less than 72% Cl<sub>3</sub>-Aba observed for chlorination reactions under similar conditions. Unlike trichlorination, incorporating a ferredoxin-based biological reductant in our tribromination assay did not enhance the yield of the tribrominated product, reaffirming the difficulty of accomplishing bromination and suggesting the role of redox potential effects (Figure S26). To verify our multibrominated analytes' identity, we obtained accurate mass spectra of these products. For the Br<sub>2</sub>-Aba species, we observe a match between the theoretical and experimental isotopic distribution patterns and a monoisotopic mass error of 0.7 ppm (Figure 4c). Comparison between the experimental and theoretical Br<sub>3</sub>-Aba accurate mass spectra gives good agreement for the isotopic distribution pattern and a monoisotopic mass error of 0.0 ppm (Figure 4d). Moreover, we confirmed C<sub>4</sub> of Aba as the site of functionalization for multibromination using the deuteriumlabeled SyrB1-Ppt-3,3-D2-Aba substrate similar to our chlorination studies (Figures S27 and S28). Our studies

ACS Catalysis pubs.acs.org/acscatalysis Research Article

suggest that for both  $Br_2$ -Aba and  $Br_3$ -Aba, all bromine atoms were installed at  $C_4$  and the regioselective outcome of C-H functionalization does not differ between the native chlorination and non-native bromination reactions. To highlight the utility of such multibrominated amino acid products, we performed dehydrohalogenation of SyrB2-generated  $Br_2$ -Aba to ETG, an alkyne analogue useful for click chemistry reactions and easily detected via an azide—alkyne cycloaddition (CuAAc) click reaction with CalFluor 488 Azide (Figure 4e,f). Ultimately, these studies mark the first instance of an iron halogenase exhibiting multibromination activity, which further broadens their already diverse catalytic repertoires.

#### CONCLUSIONS

The ability of iron halogenases to chlorinate unactivated C(sp<sup>3</sup>)-H bonds with high chemo- and regioselectivity is highly desirable from a chemical synthesis perspective. We demonstrate how the degree of halogenation can be controlled in SyrB2 halogenases to obtain chemo- and regioselective multihalogenation of Aba, likely due to the proximal positioning of C4 toward the chloro ligand over the oxo ligand of the reactive chloroferryl intermediate. Our studies reveal unprecedented trichlorination (aided by the use of a biological reductant system) and multibromination activity in SyrB2, expanding the catalytic prowess of iron halogenases. From a mechanistic perspective, we discuss the importance of the substrate's C-C bond rotational flexibility at the site of C-H functionalization in controlling the degree of halogenation. From a chemical synthesis perspective, our findings reveal the utility of iron halogenases toward late-stage multi-C-H functionalization. Insights gained from our work on controlling the degree of C–H functionalization could find use in other C–H functionalizing metalloenzymes as well.  $^{88-93}$  Overall, molecular insights gained from our work have the potential to guide the design of next-generation high-performance multihalogenation biocatalysts.

# ASSOCIATED CONTENT

## Supporting Information

The Supporting Information is available free of charge at https://pubs.acs.org/doi/10.1021/acscatal.4c02816.

Materials and methods, UPLC-MRM chromatograms, reaction cycle of 2OG-dependent nonheme iron halogenases, accurate mass spectra of analytes, bond-dissociation energy DFT-calculated energies, distance distribution of Aba C<sub>4</sub> hydrogens to the haloferryl intermediate, possible hydroxamate reaction products, and multibromination analysis with the Fdx/FdxR reduction system (PDF)

# AUTHOR INFORMATION

# **Corresponding Authors**

Anoop R. Damodaran – Department of Chemistry, University of Minnesota, Twin Cities Minneapolis, Minneapolis, Minnesota 55455, United States; Email: rdanoop@umn.edu

Ambika Bhagi-Damodaran — Department of Chemistry, University of Minnesota, Twin Cities Minneapolis, Minneapolis, Minnesota 55455, United States; orcid.org/ 0000-0002-4901-074X; Email: ambikab@umn.edu

#### **Authors**

R. Hunter Wilson – Department of Chemistry, University of Minnesota, Twin Cities Minneapolis, Minneapolis, Minnesota 55455, United States

Sourav Chatterjee – Department of Chemistry, University of Minnesota, Twin Cities Minneapolis, Minneapolis, Minnesota 55455, United States

Elizabeth R. Smithwick – Department of Chemistry, University of Minnesota, Twin Cities Minneapolis, Minneapolis, Minnesota 55455, United States

Complete contact information is available at: https://pubs.acs.org/10.1021/acscatal.4c02816

#### **Author Contributions**

R.H.W. performed protein expression and purifications, halogenation assays, accurate mass measurements, DFT calculations, and the MD simulations. R.H.W. and E.R.S. conducted the UPLC/MRM analysis. S.C. performed the reactions for alkyne generation and detection. R.H.W., A.R.D., and A.B.D. designed the study and wrote the manuscript. A.R.D. and A.B.D. supervised the research. All authors have given approval to the final version of the manuscript.

#### Notes

The authors declare no competing financial interest.

#### ACKNOWLEDGMENTS

E.R.S. and R.H.W. acknowledge the support of the National Institute of Health Chemical Biology Training Grant (T32GM132029). This work was supported by NSF CBET and CLP (grant # 2046527). Mass spectrometry analysis was performed at The University of Minnesota Department of Chemistry Mass Spectrometry Laboratory (MSL), supported by the Office of the Vice President of Research, College of Science and Engineering, and the Department of Chemistry at the University of Minnesota. The content of this paper is the sole responsibility of the authors and does not represent endorsement by MSL personnel. The authors would like to thank Profs. Krebs and Bollinger (Penn State) for providing SyrB1, SyrB2, and Sfp plasmids and Prof. Balskus (MIT) for providing TycF plasmid.

#### ABBREVIATIONS

2OG 2-oxoglutarate ACP acyl-carrier protein Ppt phosphopantetheine

Aba  $\alpha$ -aminobutyric acid MD molecular dynamics

AQC 6-aminoquinolyl-n-hydroxysuccinimidyl carbamate

MRM multiple reaction monitoring

# **■** REFERENCES

- (1) Bell, E. L.; Finnigan, W.; France, S. P.; Green, A. P.; Hayes, M. A.; Hepworth, L. J.; Lovelock, S. L.; Niikura, H.; Osuna, S.; Romero, E.; Ryan, K. S.; Turner, N. J.; Flitsch, S. L. Biocatalysis. *Nat. Rev. Methods Primers* **2021**, *1* (1), 46.
- (2) Chang, W.; Guo, Y.; Wang, C.; Butch, S. E.; Rosenzweig, A. C.; Boal, A. K.; Krebs, C.; Bollinger, J. M. Mechanism of the C5 Stereoinversion Reaction in the Biosynthesis of Carbapenem Antibiotics. *Science* **2014**, 343 (6175), 1140–1144.
- (3) McDonough, M. A.; Li, V.; Flashman, E.; Chowdhury, R.; Mohr, C.; Liénard, B. M. R.; Zondlo, J.; Oldham, N. J.; Clifton, I. J.; Lewis, J.; McNeill, L. A.; Kurzeja, R. J. M.; Hewitson, K. S.; Yang, E.; Jordan, S.; Syed, R. S.; Schofield, C. J. Cellular Oxygen Sensing: Crystal

- Structure of Hypoxia-Inducible Factor Prolyl Hydroxylase (PHD2). *Proc. Natl. Acad. Sci. U.S.A.* **2006**, *103* (26), 9814–9819.
- (4) Bollinger, J. M., Jr.; Price, J. C.; Hoffart, L. M.; Barr, E. W.; Krebs, C. Mechanism of Taurine: α-Ketoglutarate Dioxygenase (TauD) from Escherichia Coli. *Eur. J. Inorg. Chem.* **2005**, 2005 (21), 4245–4254.
- (5) Dunham, N. P.; Mitchell, A. J.; Del Río Pantoja, J. M.; Krebs, C.; Bollinger, J. M., Jr.; Boal, A. K.  $\alpha$ -Amine Desaturation of d-Arginine by the Iron(II)- and 2-(Oxo)Glutarate-Dependent l-Arginine 3-Hydroxylase, VioC. *Biochemistry* **2018**, *57* (46), 6479–6488.
- (6) Dunham, N. P.; Chang, W.; Mitchell, A. J.; Martinie, R. J.; Zhang, B.; Bergman, J. A.; Rajakovich, L. J.; Wang, B.; Silakov, A.; Krebs, C.; Boal, A. K.; Bollinger, J. M., Jr. Two Distinct Mechanisms for C–C Desaturation by Iron(II)- and 2-(Oxo)Glutarate-Dependent Oxygenases: Importance of  $\alpha$ -Heteroatom Assistance. *J. Am. Chem. Soc.* **2018**, *140* (23), 7116–7126.
- (7) Kim, W.; Chen, T.-Y.; Cha, L.; Zhou, G.; Xing, K.; Canty, N. K.; Zhang, Y.; Chang, W. Elucidation of Divergent Desaturation Pathways in the Formation of Vinyl Isonitrile and Isocyanoacrylate. *Nat. Commun.* **2022**, *13* (1), 5343.
- (8) Liu, P.; Mehn, M. P.; Yan, F.; Zhao, Z.; QueLiu, L. H. w.; Liu, H. Oxygenase Activity in the Self-Hydroxylation of (S)-2-Hydroxypropylphosphonic Acid Epoxidase Involved in Fosfomycin Biosynthesis. *J. Am. Chem. Soc.* **2004**, *126* (33), 10306–10312.
- (9) Li, J.; Liao, H.-J.; Tang, Y.; Huang, J.-L.; Cha, L.; Lin, T.-S.; Lee, J. L.; Kurnikov, I. V.; Kurnikova, M. G.; Chang, W.; Chan, N.-L.; Guo, Y. Epoxidation Catalyzed by the Nonheme Iron(II)- and 2-Oxoglutarate-Dependent Oxygenase, AsqJ: Mechanistic Elucidation of Oxygen Atom Transfer by a Ferryl Intermediate. *J. Am. Chem. Soc.* 2020, 142 (13), 6268–6284.
- (10) Busby, R. W.; Townsend, C. A. A Single Monomeric Iron Center in Clavaminate Synthase Catalyzes Three Nonsuccessive Oxidative Transformations. *Bioorg. Med. Chem.* **1996**, 4 (7), 1059–1064
- (11) Cha, L.; Paris, J. C.; Zanella, B.; Spletzer, M.; Yao, A.; Guo, Y.; Chang, W. Mechanistic Studies of Aziridine Formation Catalyzed by Mononuclear Non-Heme Iron Enzymes. *J. Am. Chem. Soc.* **2023**, *145* (11), 6240–6246.
- (12) Vaillancourt, F. H.; Yin, J.; Walsh, C. T. SyrB2 in Syringomycin E Biosynthesis Is a Nonheme FeII  $\alpha$ -Ketoglutarate- and O2-Dependent Halogenase. *Proc. Natl. Acad. Sci. U.S.A.* **2005**, 102 (29), 10111–10116.
- (13) Jiang, W.; Heemstra, J. R., Jr.; Forseth, R. R.; Neumann, C. S.; Manaviazar, S.; Schroeder, F. C.; Hale, K. J.; Walsh, C. T. Biosynthetic Chlorination of the Piperazate Residue in Kutzneride Biosynthesis by KthP. *Biochemistry* **2011**, *50* (27), 6063–6072.
- (14) Vaillancourt, F. H.; Vosburg, D. A.; Walsh, C. T. Dichlorination and Bromination of a Threonyl-S-Carrier Protein by the Non-Heme FeII Halogenase SyrB2. *ChemBioChem* **2006**, *7* (5), 748–752.
- (15) Ueki, M.; Galonić, D. P.; Vaillancourt, F. H.; Garneau-Tsodikova, S.; Yeh, E.; Vosburg, D. A.; Schroeder, F. C.; Osada, H.; Walsh, C. T. Enzymatic Generation of the Antimetabolite γ,γ-Dichloroaminobutyrate by NRPS and Mononuclear Iron Halogenase Action in a Streptomycete. *Chem. Biol.* **2006**, *13* (11), 1183–1191.
- (16) Neugebauer, M. E.; Sumida, K. H.; Pelton, J. G.; McMurry, J. L.; Marchand, J. A.; Chang, M. C. Y. A Family of Radical Halogenases for the Engineering of Amino-Acid-Based Products. *Nat. Chem. Biol.* **2019**, *15* (10), 1009–1016.
- (17) Kissman, E. N.; Neugebauer, M. E.; Sumida, K. H.; Swenson, C. V.; Sambold, N. A.; Marchand, J. A.; Millar, D. C.; Chang, M. C. Y. Biocatalytic Control of Site-Selectivity and Chain Length-Selectivity in Radical Amino Acid Halogenases. *Proc. Natl. Acad. Sci. U.S.A.* 2023, 120 (12), No. e2214512120.
- (18) Ramaswamy, A. V.; Sorrels, C. M.; Gerwick, W. H. Cloning and Biochemical Characterization of the Hectochlorin Biosynthetic Gene Cluster from the Marine Cyanobacterium Lyngbya Majuscula. *J. Nat. Prod.* **2007**, *70* (12), 1977–1986.
- (19) Pratter, S. M.; Ivkovic, J.; Birner-Gruenberger, R.; Breinbauer, R.; Zangger, K.; Straganz, G. D. More than Just a Halogenase:

- Modification of Fatty Acyl Moieties by a Trifunctional Metal Enzyme. *ChemBioChem* **2014**, *15* (4), 567–574.
- (20) Galonić, D. P.; Vaillancourt, F. H.; Walsh, C. T. Halogenation of Unactivated Carbon Centers in Natural Product Biosynthesis: Trichlorination of Leucine during Barbamide Biosynthesis. *J. Am. Chem. Soc.* **2006**, *128* (12), 3900–3901.
- (21) Galonić, D. P.; Barr, E. W.; Walsh, C. T.; Bollinger, J. M.; Krebs, C. Two Interconverting Fe(IV) Intermediates in Aliphatic Chlorination by the Halogenase CytC3. *Nat. Chem. Biol.* **2007**, 3 (2), 113–116.
- (22) Galonić Fujimori, D.; Barr, E. W.; Matthews, M. L.; Koch, G. M.; Yonce, J. R.; Walsh, C. T.; Bollinger, J. M., Jr.; Krebs, C.; Riggs-Gelasco, P. J. Spectroscopic Evidence for a High-Spin Br-Fe(IV)-Oxo Intermediate in the  $\alpha$ -Ketoglutarate-Dependent Halogenase CytC3 from Streptomyces. *J. Am. Chem. Soc.* **2007**, *129* (44), 13408–13409.
- (23) Zhu, Q.; Hillwig, M. L.; Doi, Y.; Liu, X. Aliphatic Halogenase Enables Late-Stage C—H Functionalization: Selective Synthesis of a Brominated Fischerindole Alkaloid with Enhanced Antibacterial Activity. *ChemBioChem* **2016**, *17* (6), 466–470.
- (24) Chang, Z.; Flatt, P.; Gerwick, W. H.; Nguyen, V.-A.; Willis, C. L.; Sherman, D. H. The Barbamide Biosynthetic Gene Cluster: A Novel Marine Cyanobacterial System of Mixed Polyketide Synthase (PKS)-Non-Ribosomal Peptide Synthetase (NRPS) Origin Involving an Unusual Trichloroleucyl Starter Unit. *Gene* **2002**, 296 (1–2), 235–247.
- (25) Hillwig, M. L.; Liu, X. A New Family of Iron-Dependent Halogenases Acts on Freestanding Substrates. *Nat. Chem. Biol.* **2014**, *10* (11), 921–923.
- (26) Hillwig, M. L.; Zhu, Q.; Ittiamornkul, K.; Liu, X. Discovery of a Promiscuous Non-Heme Iron Halogenase in Ambiguine Alkaloid Biogenesis: Implication for an Evolvable Enzyme Family for Late-Stage Halogenation of Aliphatic Carbons in Small Molecules. *Angew. Chem., Int. Ed.* **2016**, *55* (19), 5780–5784.
- (27) Orjala, J.; Gerwick, W. H. Barbamide, a Chlorinated Metabolite with Molluscicidal Activity from the Caribbean Cyanobacterium Lyngbya Majuscula. *J. Nat. Prod.* **1996**, *59* (4), 427–430.
- (28) Ullrich, M.; Bender, C. L. The Biosynthetic Gene Cluster for Coronamic Acid, an Ethylcyclopropyl Amino Acid, Contains Genes Homologous to Amino Acid-Activating Enzymes and Thioesterases. *J. Bacteriol.* **1994**, *176* (24), 7574–7586.
- (29) Zhang, H.; Kakeya, H.; Osada, H. Biosynthesis of 1-Aminocyclopropane-1-Carboxylic Acid Moiety on Cytotrienin A in Streptomyces Sp. *Tetrahedron Lett.* **1998**, 39 (38), 6947–6948.
- (30) Chung, W.; Vanderwal, C. D. Stereoselective Halogenation in Natural Product Synthesis. *Angew. Chem., Int. Ed.* **2016**, *55* (14), 4396–4434
- (31) Landry, M. L.; Burns, N. Z. Catalytic Enantioselective Dihalogenation in Total Synthesis. *Acc. Chem. Res.* **2018**, *51* (5), 1260–1271.
- (32) Dong, J.; Fernández-Fueyo, E.; Hollmann, F.; Paul, C. E.; Pesic, M.; Schmidt, S.; Wang, Y.; Younes, S.; Zhang, W. Biocatalytic Oxidation Reactions: A Chemist's Perspective. *Angew. Chem., Int. Ed.* **2018**, *57* (30), 9238–9261.
- (33) Das, R.; Kapur, M. Transition-Metal-Catalyzed Site-Selective C-H Halogenation Reactions. *Asian J. Org. Chem.* **2018**, 7 (8), 1524–1541.
- (34) Scheide, M. R.; Nicoleti, C. R.; Martins, G. M.; Braga, A. L. Electrohalogenation of Organic Compounds. *Org. Biomol. Chem.* **2021**, *19* (12), 2578–2602.
- (35) Nanjo, T.; Matsumoto, A.; Oshita, T.; Takemoto, Y. Synthesis of Chlorinated Oligopeptides via  $\gamma$  and  $\delta$ -Selective Hydrogen Atom Transfer Enabled by the N-Chloropeptide Strategy. *J. Am. Chem. Soc.* **2023**, *145*, 19067–19075.
- (36) Liang, L.; Guo, L.-D.; Tong, R. Achmatowicz Rearrangement-Inspired Development of Green Chemistry, Organic Methodology, and Total Synthesis of Natural Products. *Acc. Chem. Res.* **2022**, *55* (16), 2326–2340.

- (37) Fu, N.; Sauer, G. S.; Lin, S. Electrocatalytic Radical Dichlorination of Alkenes with Nucleophilic Chlorine Sources. *J. Am. Chem. Soc.* **2017**, *139* (43), 15548–15553.
- (38) Sauer, G. S.; Lin, S. An Electrocatalytic Approach to the Radical Difunctionalization of Alkenes. *ACS Catal.* **2018**, *8* (6), 5175–5187.
- (39) Seidl, F. J.; Min, C.; Lopez, J. A.; Burns, N. Z. Catalytic Regioand Enantioselective Haloazidation of Allylic Alcohols. *J. Am. Chem. Soc.* **2018**, *140* (46), 15646–15650.
- (40) Lian, P.; Long, W.; Li, J.; Zheng, Y.; Wan, X. Visible-Light-Induced Vicinal Dichlorination of Alkenes through LMCT Excitation of CuCl2. *Angew. Chem., Int. Ed.* **2020**, *59* (52), 23603–23608.
- (41) Sarie, J. C.; Neufeld, J.; Daniliuc, C. G.; Gilmour, R. Catalytic Vicinal Dichlorination of Unactivated Alkenes. *ACS Catal.* **2019**, 9 (8), 7232–7237.
- (42) Bai, Y.; Li, Y.; Zhang, Z.; Yang, X.; Zhang, J.; Chen, L.; Li, Y.; Zeng, X.; Zhang, M. Regioselective Difunctionalization of Alkene: A Simple Access to Haloether, Haloesters and Halohydrins. *Tetrahedron Lett.* **2022**, *101*, 153923.
- (43) Cui, H.; Shen, Y.; Chen, Y.; Wang, R.; Wei, H.; Fu, P.; Lei, X.; Wang, H.; Bi, R.; Zhang, Y. Two-Stage Syntheses of Clionastatins A and B. J. Am. Chem. Soc. 2022, 144 (20), 8938–8944.
- (44) Jayaraman, A.; Cho, E.; Irudayanathan, F. M.; Kim, J.; Lee, S. Metal-Free Decarboxylative Trichlorination of Alkynyl Carboxylic Acids: Synthesis of Trichloromethyl Ketones. *Adv. Synth. Catal.* **2018**, 360 (1), 130–141.
- (45) Li, X.; Jin, J.; Chen, P.; Liu, G. Catalytic Remote Hydrohalogenation of Internal Alkenes. *Nat. Chem.* **2022**, *14* (4), 425–432.
- (46) Bian, M.; Zhou, J. f.; Tang, D. m. Facile Approach to Geminal Heterodihalogenation. One-Pot Synthesis of  $\alpha$ -Bromo- $\alpha$ -Chloro Ketones. *Synlett* **2020**, *31* (14), 1430–1434.
- (47) Gallucci, R. R.; Going, R. Chlorination of Aliphatic Ketones in Methanol. *J. Org. Chem.* **1981**, *46* (12), 2532–2538.
- (48) Wang, J.; Li, H.; Zhang, D.; Huang, P.; Wang, Z.; Zhang, R.; Liang, Y.; Dong, D. Divergent Synthesis of  $\alpha,\alpha$ -Dihaloamides through  $\alpha,\alpha$ -Dihalogenation of  $\beta$ -Oxo Amides by Using N-Halosuccinimides. *Eur. J. Org Chem.* **2013**, 2013 (24), 5376–5380.
- (49) Tarantino, G.; Hammond, C. Catalytic C(Sp3)-F Bond Formation: Recent Achievements and Pertaining Challenges. *Green Chem.* **2020**, 22 (16), 5195-5209.
- (50) Ren, J.; Tong, R. Convenient in Situ Generation of Various Dichlorinating Agents from Oxone and Chloride: Diastereoselective Dichlorination of Allylic and Homoallylic Alcohol Derivatives. *Org. Biomol. Chem.* **2013**, *11* (26), 4312–4315.
- (51) Jin, J.; Zhao, Y.; Kyne, S. H.; Farshadfar, K.; Ariafard, A.; Chan, P. W. H. Copper(I)-Catalysed Site-Selective C(Sp3)—H Bond Chlorination of Ketones, (E)-Enones and Alkylbenzenes by Dichloramine-T. *Nat. Commun.* **2021**, *12* (1), 4065.
- (52) Latham, J.; Henry, J.-M.; Sharif, H. H.; Menon, B. R. K.; Shepherd, S. A.; Greaney, M. F.; Micklefield, J. Integrated Catalysis Opens New Arylation Pathways via Regiodivergent Enzymatic C–H Activation. *Nat. Commun.* **2016**, *7* (1), 11873.
- (53) Petrone, D. A.; Ye, J.; Lautens, M. Modern Transition-Metal-Catalyzed Carbon-Halogen Bond Formation. *Chem. Rev.* **2016**, *116* (14), 8003–8104.
- (54) Xiong, H.-Y.; Cahard, D.; Pannecoucke, X.; Besset, T. Pd-Catalyzed Directed Chlorination of Unactivated C(Sp3)—H Bonds at Room Temperature. *Eur. J. Org Chem.* **2016**, 2016 (21), 3625–3630.
- (55) Li, G.; Dilger, A. K.; Cheng, P. T.; Ewing, W. R.; Groves, J. T. Selective C–H Halogenation with a Highly Fluorinated Manganese Porphyrin. *Angew. Chem., Int. Ed.* **2018**, *57* (5), 1251–1255.
- (56) Ozawa, J.; Kanai, M. Silver-Catalyzed C(Sp3)-H Chlorination. Org. Lett. 2017, 19 (6), 1430-1433.
- (57) Fawcett, A.; Keller, M. J.; Herrera, Z.; Hartwig, J. F. Site Selective Chlorination of C(Sp3)–H Bonds Suitable for Late-Stage Functionalization. *Angew. Chem., Int. Ed.* **2021**, *60* (15), 8276–8283.
- (58) Quinn, R. K.; Könst, Z. A.; Michalak, S. E.; Schmidt, Y.; Szklarski, A. R.; Flores, A. R.; Nam, S.; Horne, D. A.; Vanderwal, C. D.; Alexanian, E. J. Site-Selective Aliphatic C–H Chlorination Using

- N-Chloroamides Enables a Synthesis of Chlorolissoclimide. *J. Am. Chem. Soc.* **2016**, 138 (2), 696–702.
- (59) Smithwick, E. R.; Wilson, R. H.; Chatterjee, S.; Pu, Y.; Dalluge, J. J.; Damodaran, A. R.; Bhagi-Damodaran, A. Electrostatically Regulated Active Site Assembly Governs Reactivity in Nonheme Iron Halogenases. ACS Catal. 2023, 13 (20), 13743–13755.
- (60) Martinie, R. J.; Livada, J.; Chang, W.; Green, M. T.; Krebs, C.; Bollinger, J. M.; Silakov, A. Experimental Correlation of Substrate Position with Reaction Outcome in the Aliphatic Halogenase, SyrB2. *J. Am. Chem. Soc.* **2015**, 137 (21), 6912–6919.
- (61) Blasiak, L. C.; Vaillancourt, F. H.; Walsh, C. T.; Drennan, C. L. Crystal Structure of the Non-Haem Iron Halogenase SyrB2 in Syringomycin Biosynthesis. *Nature* **2006**, *440* (7082), 368–371.
- (62) Mehmood, R.; Qi, H. W.; Steeves, A. H.; Kulik, H. J. The Protein's Role in Substrate Positioning and Reactivity for Biosynthetic Enzyme Complexes: The Case of SyrB2/SyrB1. ACS Catal. 2019, 9 (6), 4930–4943.
- (63) Chen, Y.-H.; Comeaux, L. M.; Herbst, R. W.; Saban, E.; Kennedy, D. C.; Maroney, M. J.; Knapp, M. J. Coordination Changes and Auto-Hydroxylation of FIH-1: Uncoupled O2-Activation in a Human Hypoxia Sensor. *J. Inorg. Biochem.* **2008**, *102* (12), 2120–2129.
- (64) Ryle, M. J.; Koehntop, K. D.; Liu, A.; Que, L.; Hausinger, R. P. Interconversion of Two Oxidized Forms of Taurine/α-Ketoglutarate Dioxygenase, a Non-Heme Iron Hydroxylase: Evidence for Bicarbonate Binding. *Proc. Natl. Acad. Sci. U.S.A.* **2003**, *100* (7), 3790–3795.
- (65) Wong, S. D.; Srnec, M.; Matthews, M. L.; Liu, L. V.; Kwak, Y.; Park, K.; Bell III, C. B.; Alp, E. E.; Zhao, J.; Yoda, Y.; Kitao, S.; Seto, M.; Krebs, C.; Bollinger, J. M.; Solomon, E. I. Elucidation of the Fe(iv)=O intermediate in the catalytic cycle of the halogenase SyrB2. *Nature* **2013**, 499 (7458), 320–323.
- (66) Neugebauer, M. E.; Kissman, E. N.; Marchand, J. A.; Pelton, J. G.; Sambold, N. A.; Millar, D. C.; Chang, M. C. Y. Reaction Pathway Engineering Converts a Radical Hydroxylase into a Halogenase. *Nat. Chem. Biol.* **2021**, *18*, 171–179.
- (67) Liu, J.; Chakraborty, S.; Hosseinzadeh, P.; Yu, Y.; Tian, S.; Petrik, I.; Bhagi, A.; Lu, Y. Metalloproteins Containing Cytochrome, Iron–Sulfur, or Copper Redox Centers. *Chem. Rev.* **2014**, *114* (8), 4366–4469.
- (68) Kulik, H. J.; Drennan, C. L. Substrate Placement Influences Reactivity in Non-Heme Fe(II) Halogenases and Hydroxylases. *J. Biol. Chem.* **2013**, 288 (16), 11233–11241.
- (69) Borowski, T.; Noack, H.; Radoń, M.; Zych, K.; Siegbahn, P. E. M. Mechanism of Selective Halogenation by SyrB2: A Computational Study. *J. Am. Chem. Soc.* **2010**, *132* (37), 12887–12898.
- (70) Mehmood, R.; Vennelakanti, V.; Kulik, H. J. Spectroscopically Guided Simulations Reveal Distinct Strategies for Positioning Substrates to Achieve Selectivity in Nonheme Fe(II)/α-Ketoglutarate-Dependent Halogenases. ACS Catal. 2021, 11 (19), 12394–12408.
- (71) Rugg, G.; Senn, M. Formation and Structure of the Ferryl [Fe=O] Intermediate in the Non-Haem Iron Halogenase SyrB2: Classical and QM/MM Modelling Agree. *Phys. Chem. Chem. Phys.* **2017**, *19* (44), 30107–30119.
- (72) Huang, J.; Li, C.; Wang, B.; Sharon, D. A.; Wu, W.; Shaik, S. Selective Chlorination of Substrates by the Halogenase SyrB2 Is Controlled by the Protein According to a Combined Quantum Mechanics/Molecular Mechanics and Molecular Dynamics Study. ACS Catal. 2016, 6 (4), 2694–2704.
- (73) Mitchell, A. J.; Zhu, Q.; Maggiolo, A. O.; Ananth, N. R.; Hillwig, M. L.; Liu, X.; Boal, A. K. Structural Basis for Halogenation by Iron- and 2-Oxo-Glutarate-Dependent Enzyme WelO5. *Nat. Chem. Biol.* **2016**, *12* (8), 636–640.
- (74) Zhang, X.; Wang, Z.; Gao, J.; Liu, W. Chlorination versus Hydroxylation Selectivity Mediated by the Non-Heme Iron Halogenase WelO5. *Phys. Chem. Chem. Phys.* **2020**, 22 (16), 8699–8712.

- (75) Timmins, A.; Fowler, N. J.; Warwicker, J.; Straganz, G. D.; de Visser, S. P. Does Substrate Positioning Affect the Selectivity and Reactivity in the Hectochlorin Biosynthesis Halogenase? *Front. Chem.* **2018**, *6*, 513.
- (76) Srnec, M.; Solomon, E. I. Frontier Molecular Orbital Contributions to Chlorination versus Hydroxylation Selectivity in the Non-Heme Iron Halogenase SyrB2. *J. Am. Chem. Soc.* **2017**, 139 (6), 2396–2407.
- (77) Srnec, M.; Wong, S. D.; Matthews, M. L.; Krebs, C.; Bollinger, J. M.; Solomon, E. I. Electronic Structure of the Ferryl Intermediate in the  $\alpha$ -Ketoglutarate Dependent Non-Heme Iron Halogenase SyrB2: Contributions to H Atom Abstraction Reactivity. *J. Am. Chem. Soc.* **2016**, *138* (15), 5110–5122.
- (78) Kulik, H. J.; Blasiak, L. C.; Marzari, N.; Drennan, C. L. First-Principles Study of Non-Heme Fe(II) Halogenase SyrB2 Reactivity. *J. Am. Chem. Soc.* **2009**, *131* (40), 14426–14433.
- (79) Kastner, D. W.; Nandy, A.; Mehmood, R.; Kulik, H. J. Mechanistic Insights into Substrate Positioning That Distinguish Non-Heme Fe(II)/ $\alpha$ -Ketoglutarate-Dependent Halogenases and Hydroxylases. ACS Catal. 2023, 13 (4), 2489–2501.
- (80) Pandian, S.; Vincent, M. A.; Hillier, I. H.; Burton, N. Why Does the Enzyme SyrB2 Chlorinate, but Does Not Hydroxylate, Saturated Hydrocarbons? A Density Functional Theory (DFT) Study. *Dalton Trans.* **2009**, No. 31, 6201–6207. 0
- (81) Nakamura, H.; Wang, J. X.; Balskus, E. P. Assembly Line Termination in Cylindrocyclophane Biosynthesis: Discovery of an Editing Type II Thioesterase Domain in a Type I Polyketide Synthase. *Chem. Sci.* **2015**, *6* (7), 3816–3822.
- (82) Zhang, W.; Ostash, B.; Walsh, C. T. Identification of the Biosynthetic Gene Cluster for the Pacidamycin Group of Peptidyl Nucleoside Antibiotics. *Proc. Natl. Acad. Sci. U.S.A.* **2010**, *107* (39), 16828–16833.
- (83) Calderone, C. T.; Bumpus, S. B.; Kelleher, N. L.; Walsh, C. T.; Magarvey, N. A. A ketoreductase domain in the PksJ protein of the bacillaene assembly line carries out both  $\alpha$  and  $\beta$ -ketone reduction during chain growth. *Proc. Natl. Acad. Sci. U.S.A.* **2008**, *105* (35), 12809–12814.
- (84) Vaillancourt, F. H.; Yeh, E.; Vosburg, D. A.; O'Connor, S. E.; Walsh, C. T. Cryptic Chlorination by a Non-Haem Iron Enzyme during Cyclopropyl Amino Acid Biosynthesis. *Nature* **2005**, 436 (7054), 1191–1194.
- (85) Matthews, M. L.; Neumann, C. S.; Miles, L. A.; Grove, T. L.; Booker, S. J.; Krebs, C.; Walsh, C. T.; Bollinger, J. M. Substrate Positioning Controls the Partition between Halogenation and Hydroxylation in the Aliphatic Halogenase, SyrB2. *Proc. Natl. Acad. Sci. U.S.A.* 2009, 106 (42), 17723–17728.
- (86) Matthews, M. L.; Chang, W.; Layne, A. P.; Miles, L. A.; Krebs, C.; Bollinger, J. M. Direct Nitration and Azidation of Aliphatic Carbons by an Iron-Dependent Halogenase. *Nat. Chem. Biol.* **2014**, *10* (3), 209–215.
- (87) Matthews, M. L.; Krest, C. M.; Barr, E. W.; Vaillancourt, F. H.; Walsh, C. T.; Green, M. T.; Krebs, C.; Bollinger, J. M. Substrate-Triggered Formation and Remarkable Stability of the C-H Bond-Cleaving Chloroferryl Intermediate in the Aliphatic Halogenase, SyrB2. *Biochemistry* **2009**, 48 (20), 4331–4343.
- (88) Tian, J.; Liu, J.; Knapp, M.; Donnan, P. H.; Boggs, D. G.; Bridwell-Rabb, J. Custom Tuning of Rieske Oxygenase Reactivity. *Nat. Commun.* **2023**, *14* (1), 5858.
- (89) Ghirlanda, G. Design of Membrane Proteins: Toward Functional Systems. *Curr. Opin. Chem. Biol.* **2009**, *13* (5–6), 643–651
- (90) Tian, S.; Jones, S. M.; Jose, A.; Solomon, E. I. Chloride Control of the Mechanism of Human Serum Ceruloplasmin (Cp) Catalysis. *J. Am. Chem. Soc.* **2019**, *141* (27), 10736–10743.
- (91) Joseph, C. A.; Maroney, M. J. Cysteine Dioxygenase: Structure and Mechanism. *Chem. Commun.* **2007**, No. 32, 3338–3349.
- (92) Wilson, R. H.; Chatterjee, S.; Smithwick, E. R.; Dalluge, J. J.; Bhagi-Damodaran, A. Role of Secondary Coordination Sphere

- Residues in Halogenation Catalysis of Non-heme Iron Enzymes. ACS Catal. 2022, 12, 10913–10924.
- (93) Smithwick, E. R.; Bhagi-Damodaran, A.; Damodaran, A. R. *MIE* **2024**, DOI: 10.1016/bs.mie.2024.05.004.